Journal of Radioanalytical and Nuclear Chemistry (2018) 317:897–905
https://doi.org/10.1007/s10967-018-5955-5

Application of the ^{226}Ra–^{230}Th–^{234}U and ^{227}Ac–^{231}Pa–^{235}U radiochronometers to UF_6 cylinders

John M. Rolison[1] · Ross W. Williams[1]

Received: 19 March 2018 / Published online: 16 June 2018

Abstract
Uranium-series radiometric dating was performed on two well-pedigreed UF_6 cylinder samples containing highly enriched uranium that were in use at the Portsmouth Gaseous Diffusion Plant between the mid-1970s and mid-1980s. Daughter–parent (i.e. ^{231}Pa–^{235}U, ^{230}Th–^{234}U) radiometric ages determined on solid heel materials (e.g. UO_2F_2, UF_4) recovered from the emptied cylinders are unrealistically old due to the preferential sequestration of progeny isotopes relative to uranium within the solid heels. However, limited elemental fractionation amongst the progeny isotopes themselves in the heel material allowed for realistic age constraints on the fill dates of the UF_6 cylinders to be extracted from the granddaughter–daughter systems (i.e. ^{226}Ra–^{230}Th, ^{227}Ac–^{231}Pa).

Keywords U-series radiochronometry · Nuclear forensics · Uranium hexafluoride · Age-dating · Isotope dilution MC-ICP-MS

Introduction

Uranium-series radiometric dating is an important tool for establishing a timeline of nuclear material production for nuclear forensics investigations. Determining radiometric ages requires the content of progeny isotopes (i.e. ^{231}Pa, ^{230}Th, ^{227}Ac, ^{226}Ra) relative to parent isotopes (i.e. ^{235}U, ^{234}U) to be measured in the material of interest. In calculating a model age, it is assumed that (1) the material was initially produced free of all progeny isotopes and (2) that the material remained a closed system between the time of its initial production and the time it was analyzed, such that the radioactive decay of the parent isotopes was the only source of the progeny isotopes. Under these model assumptions, a *model age* of the material can be determined by solving Bateman's equations of radioactive decay [1] using the known decay constants for the U-series isotopes. The determination of multiple model ages using different radiochronometers (daughter–parent or granddaughter–parent pairs) provides a strong test of whether or not the model assumptions hold true for a particular material of unknown origin.

There are numerous examples in the literature of different nuclear materials that have been shown to follow the model assumptions of radiometric dating mentioned above for the daughter-parent system (e.g. [2, 3]) and the granddaughter–parent system (e.g. [4, 5]). These are important observations because they demonstrate that the assumptions made in radiometric dating of uranium materials are valid in many cases. However, radiometric dating of residual solid material extracted from emptied UF_6 cylinders used for storing and transporting U presents a major technical issue. While most U exists in cylinders as UF_6, some UF_6 decomposes through radiolysis and hydrolysis to form a solid deposit (e.g. UF_4, UO_2F_2) that is known as 'heel' material [6]. Unlike UF_6, the heel material does not sublime upon heating of the cylinder and is therefore not removed from a cylinder when emptied via gas transfer. Although the total amount of U contained in the heel material is relatively minor compared to the total U in the cylinder, it is expected that nearly all of the progeny isotopes produced by the radioactive decay of U are sequestered in the heel material because these elements do not form a volatile hexafluoride compound (Fig. 1). Thus,

✉ John M. Rolison
rolison2@llnl.gov

[1] Nuclear and Chemical Sciences Division, Physical and Life Sciences Directorate, Lawrence Livermore National Laboratory, 7000 East Avenue, Livermore, CA 94551, USA

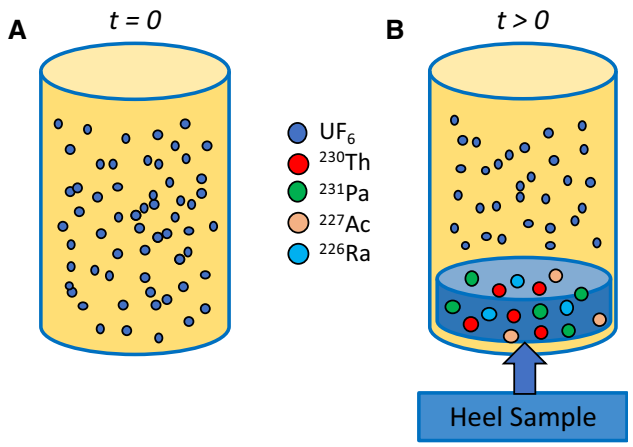

Fig. 1 Schematic representation of the expected behavior of U, Th, Pa, Ac, and Ra in a UF_6 cylinder. **a** When the cylinder is initially filled ($t = 0$), only U is present and is in the form of UF_6 (blue circles). **b** Over time (i.e. $t > 0$), some of the UF_6 decomposes through radiolysis and hydrolysis to form a solid deposit (e.g. UF_4, UO_2F_2; blue disk) which sequesters the ingrown ^{231}Pa, ^{230}Th, ^{227}Ac, and ^{226}Ra. The solid deposit, i.e. heel material, is what is sampled and analyzed for radiometric dating purposes. (Color figure online)

there is elemental fractionation between the parent and progeny isotopes, which nullifies the primary radiometric dating assumption that material has remained a closed system. Furthermore, UF_6 cylinders can be filled, emptied either entirely or partially of the UF_6, and possibly refilled, which will also act to nullify the assumption of closed system behavior. It is expected that the heel material formed in UF_6 cylinders will contain excess progeny isotopes relative to the content of the parent isotopes which will result in the calculation of an artificially older model age of the heel material than would be expected, assuming the fill date of the cylinder is taken as initial production date of the material ($t = 0$) and that the UF_6 was free of progeny isotopes when the cylinder was filled.

In this study, the application of the granddaughter-daughter radiometric dating of UF_6 cylinder samples is investigated. While it is expected that progeny isotopes (i.e. ^{231}Pa, ^{230}Th, ^{227}Ac, ^{226}Ra) are significantly fractionated from their parent isotopes (i.e. ^{235}U, ^{234}U) in UF_6 cylinders, there should be limited elemental fractionation amongst the different progeny isotopes themselves such that the $^{227}Ac/^{231}Pa$ and $^{226}Ra/^{230}Th$ ratios may still provide useful age information. The UF_6 cylinders investigated in this study are reasonably well pedigreed and thus provide an opportunity to develop a framework with which to interpret radiometric ages in an isotopically open system.

Samples

Two UF_6 cylinders (G-03-0146 and G-03-0291) were selected for analysis in this study. They are both 2S cylinders, which can contain up to ~ 1.5 kg of highly enriched uranium (HEU) or ~ 2.2 kg of UF_6 [6]. Both cylinders were initially filled at the Portsmouth Gaseous Diffusion Plant (PORTS) presumably with HEU derived from the Portsmouth cascade, and were used as analytical standards in the Portsmouth Plant Analytical Laboratory (Table 1). The initial fill dates of the two cylinders are only known approximately from notes taken in Portsmouth Plant Analytical Laboratory log books and from interviews with current and former Portsmouth Plant Analytical Laboratory employees [7]. The fill date of cylinder G-03-0146 was around June 1977 while the fill date of G-03-0291 was around March 1987 (Table 1). The fill dates are estimated from the earliest available documentation of the subsampling and/or analysis of the material by the Portsmouth Plant Analytical Laboratory. The dates of subsampling into Hoke tubes and/or analyses at the Portsmouth Plant Analytical Laboratory are thought to be within a few months from when the cylinders were initially filled [7]).

Cylinders G-03-0146 and G-03-0291 are from a set of 97 2S cylinders containing PORTS HEU that were sent to Nuclear Fuels Services (NFS) in Erwin, Tennessee to be disposed of by conversion to low enriched uranium. A subset of five cylinders, including G-03-0146 and G-03-0291, were selected for retention, sampling, and analysis by the United States Department of Energy because they were most likely to be representative of the contemporaneously produced PORTS HEU product. Cylinders G-03-0146 and G-03-0291 were shipped from PORTS to NFS and were subsequently emptied of their bulk UF_6 via gas transfer with slight heating. The date on which the UF_6 was removed and the amount of UF_6 removed at NFS is presented in Table 2. The amount of UF_6 removed from cylinder G-03-0146 was ~ 10 g, whereas more than 1 kg of UF_6 removed from cylinder G-03-0291. Thus, cylinder G-03-0146 was already nearly empty while cylinder G-03-0291 was approximately half full when received at NFS. The time between the initial fill date at PORTS and final empty date at NFS was ~ 35 years for cylinder G-03-0146 and ~ 25 years for cylinder G-03-0291.

After NFS emptied the bulk of the remaining UF_6, cylinders G-03-0146 and G-03-0291 were shipped to Materials and Chemistry Laboratory, Inc. (MCL; Oak Ridge, Tennessee). The residual UF_6 (~ 10 g) contained within the cylinders was removed via gas transfer and stored in smaller P10 tubes for shipping to different laboratories. After fully emptying the cylinders of residual UF_6, the cylinders were opened by sawing off the top of the

Table 1 Uranium isotope composition of the two UF_6 cylinders as determined by the Portsmouth Plant Analytical Lab

Cylinder ID	^{234}U mass%	^{235}U mass%	^{236}U mass%	^{238}U mass%	Date of earliest PORTS sampling	Date of earliest PORTS analysis
G-03-0146	0.7059	91.846	0.1155	7.333	20-Jun-77	21-Jul-77
G-03-0291	0.8577	90.709	0.0215	8.412	Unknown	17-Mar-87

Table 2 Mass of UF_6 removed at NFS

Cylinder ID	Date of transfer at NFS	Net mass before UF_6 removal (g)	Net mass after removal (g)
G-03-0146	22-Nov-11	99.8	88
G-03-0291	26-Jan-12	1067.5	52

cylinder using a circular saw fitted with a diamond blade installed inside a glove box (Fig. 2; [7]). After the cylinder was cut into two pieces, the 'loose' heel material was emptied from the cylinder and collected for distribution to different laboratories. The heel material collected at MCL was only what was considered 'loose', meaning that it could easily be poured out of the cylinder half. The inside walls of the cylinders were inspected at MCL for any corrosion products or heel material that was stuck to the inside walls, but no such material was observed in significant quantity [7]. Therefore the 'loose' heel material was the only material recovered by MCL. The amount of loose heel material recovered at MCL was approximately 40 g from each cylinder.

Some of the loose heel material and associated cylinder halves were then shipped to Oak Ridge National Laboratory (ORNL) before finally being shipped to Lawrence Livermore National Laboratory (LLNL) in 2016. Once received at LLNL, the inside walls of cylinders G-03-0146 and G-03-0291 were scraped with a spatula and the material that was released from the walls was collected and termed 'cylinder wall deposits'. Thus, each cylinder

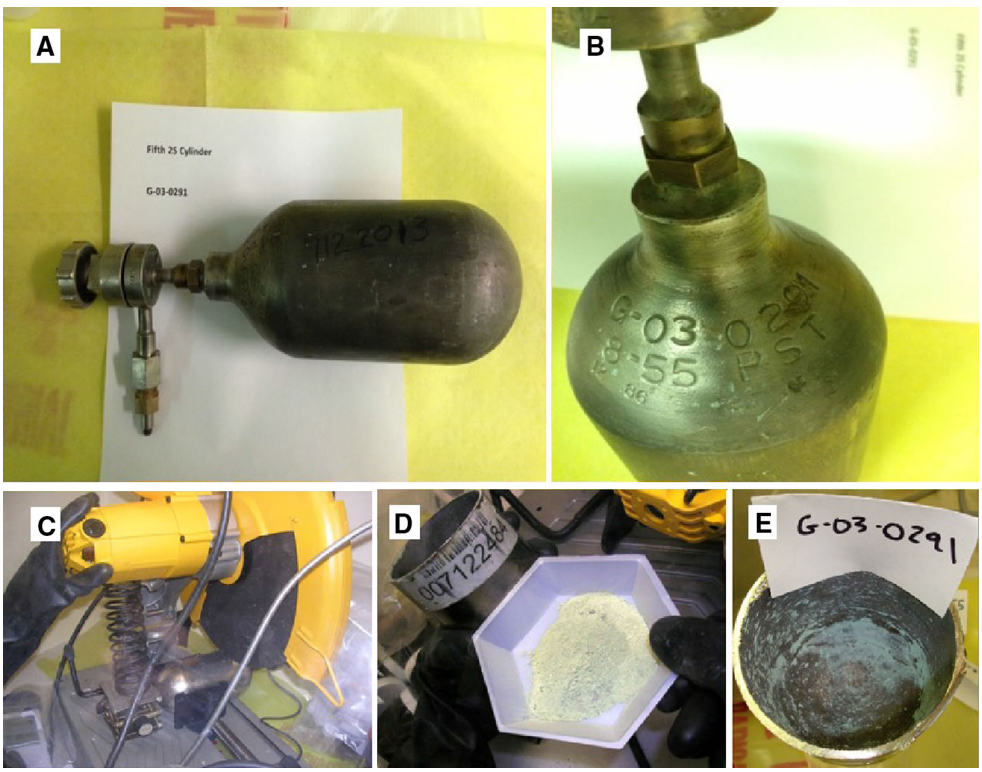

Fig. 2 Images taken at the time of open the cylinders. Used with permission from Materials and Chemistry Laboratory, Inc. (Oak Ridge, Tennessee). **a** Image of cylinder G-03-0291 shown next to a piece of letter sized printer paper for scale. **b** Image of the inscribed label on cylinder G-03-0291. **c** Mounted circular saw with a diamond blade installed inside a glove box with a 2S cylinder being sawed open. **d** Recovered loose heel material from an opened 2S cylinder. **e** Bottom half of cylinder G-03-0291 after the loose heels were removed but with clearly visible wall deposits still remaining

yielded two samples each, one loose heel sample and one wall deposit, for a total of four samples. The samples are labeled G-03-0146-LH, G-03-0146-CWD, G-03-0291-LH, and G-03-0291-CWD, with LH indicating loose heel and CWD indicating cylinder wall deposit. Both material types are fine powders that were easily dispersible. Handling of the solid loose heels and wall deposits was performed inside a disposable glove bag set up within a fume hood at LLNL.

Experimental

Sample digestion

All acids used in this study were ultra-high purity grade (Baseline®, Seastar Chemicals Inc.). All water used for dilutions and rinsing of lab ware was > 18.2 MΩ (Milli-Q®, Millipore). Approximately 200 mg of each sample was transferred to a quartz tube, weighed, and subsequently digested with 2 mL 8 M HNO_3 while being heated on a hot plate at ~ 120 °C. After the reaction subsided, the solution was transferred with multiple rinses of the quartz tube to a pre-weighted 30 mL Savillex perfluoroalkoxy vial and diluted to approximately 20 mL total volume with 4 M HNO_3 + 0.005 M HF, with a final weight of the full vial being recorded.

Analysis of U, Pa, Th, Ac, and Ra

The concentrations of the elements and isotopes of interest in the final solution were determined via isotope dilution multi-collector inductively coupled plasma mass spectrometry (MC-ICP-MS). The analytical methods used at LLNL have been extensively documented [2–5] and are thus only briefly discussed here. Separate aliquots of the samples were taken for the analysis of U isotope composition, U concentration, paired ^{231}Pa and ^{230}Th concentrations, and paired ^{227}Ac and ^{226}Ra concentrations. All aliquots, except for the U isotope composition aliquot, were spiked with appropriate isotope dilution tracers. The different spikes used were as follows: a ^{233}U spike for U concentration, a ^{233}Pa spike for ^{231}Pa concentration, a ^{229}Th spike for ^{230}Th concentration, a ^{225}Ac spike for ^{227}Ac concentration, and a ^{228}Ra spike for ^{226}Ra concentration. After spiking, the samples were sealed and fluxed on a hotplate to reach isotopic equilibrium. All aliquots were then subjected to ion-exchange chromatography to separate and purify the target element(s) from each aliquot. The details of the spike calibrations and chemical separation procedures can be found elsewhere [2–5]. The purified samples were then analyzed on the Nu Instruments Nu Plasma HR MC-ICP-MS at LLNL following methods presented in Rolison et al. [5] and references therein. Instrumental mass bias and electron multiplier efficiencies were corrected by bracketing sets of three samples with analyses of NBL CRM U010, which is a uranium certified reference material issued by New Brunswick Laboratory. Quality control of the instrumental mass bias and electron multiplier efficiencies corrections was established through the repeated analysis of NBL CRM U005A. Furthermore, multiple NBL uranium certified reference materials were chemically processed and analyzed alongside the UF_6 cylinder samples during the course of the analytical campaign. The NBL CRMs analyzed were CRM 125-A, CRM U050, CRM U100, and CRM U630. Radiometric ages for these NBL CRMs were determined using the ^{231}Pa–^{235}U, ^{230}Th–^{234}U, ^{227}Ac–^{235}U or ^{226}Ra–^{234}U radiochronometers. In all cases, the radiometric ages were in agreement with the certified model ages or known purifications dates [5].

Results and discussion

The analytical results obtained at LLNL are presented in Tables 3, 4 and 5. Both cylinders contain HEU with > 90% ^{235}U and also contain ^{236}U (Table 3). The U isotope composition determined at LLNL for the two cylinders is in agreement with the U isotope composition for these cylinders reported by the Portsmouth Plant Analytical Laboratory. Furthermore, the two sample types, loose heels and cylinder wall deposits, yield identical U isotope composition within the same cylinder. The concentrations of the individual uranium isotopes in the primary dissolution solution range between 10^{15} and 10^{18} atoms g^{-1}, and are variable due to different amounts of solid material used for the dissolutions (Table 4). The progeny isotopes in the primary solutions are around 10^{12} atoms g^{-1} ^{231}Pa, 10^{14} atoms g^{-1} ^{230}Th, 10^{9} atoms g^{-1} ^{227}Ac, and 10^{10} atoms g^{-1} ^{226}Ra (Table 5). The precision on each measurement is the combined standard uncertainty (U) with a coverage factor of $k = 2$. In most cases, the uncertainty in the final concentration is dominated by the uncertainty in the calibration of the isotope dilution tracer which is ultimately limited by the precision assigned to the reference material used to calibrate the tracer.

The results obtained for cylinders G-03-0146 and G-03-0291 allow for radiometric model ages to be calculated based on the different ratios of progeny to parent isotopes (Tables 6, 7). The ^{231}Pa–^{235}U and ^{230}Th–^{234}U radiochronometers yield ages of > 400 years for cylinder G-03-0146 and > 700 years for cylinder G-03-0291. Similarly, unrealistic results are obtained for the ^{227}Ac–^{235}U and ^{226}Ra–^{234}U radiochronometers. These ages are clearly far too old to be realistic and demonstrate that the progeny

Table 3 Uranium isotope composition of the UF_6 cylinder samples

Sample ID	$^{234}U/^{238}U$	$^{235}U/^{238}U$	$^{236}U/^{238}U$
G-03-0146-LH	0.09767 ± 0.00020	12.666 ± 0.014	0.015927 ± 0.000057
G-03-0146-CWD	0.09764 ± 0.00023	12.658 ± 0.014	0.015943 ± 0.000051
G-03-0291-LH	0.10338 ± 0.00014	10.903 ± 0.012	0.002377 ± 0.000016
G-03-0291-CWD	0.10339 ± 0.00019	10.899 ± 0.012	0.002374 ± 0.000032

Uncertainties represent expanded uncertainties with a coverage factor of $k = 2$

Table 4 Concentration of U isotopes in the primary dissolution solution

Sample ID	^{234}U (atoms g^{-1})	^{235}U (atoms g^{-1})	^{236}U (atoms g^{-1})	^{238}U (atoms g^{-1})
G-03-0146-LH	$(6.0590 \pm 0.0091) \times 10^{16}$	$(7.8574 \pm 0.0098) \times 10^{18}$	$(9.880 \pm 0.021) \times 10^{15}$	$(6.2037 \pm 0.0069) \times 10^{17}$
G-03-0146-CWD	$(1.1485 \pm 0.0019) \times 10^{17}$	$(1.4889 \pm 0.0018) \times 10^{19}$	$(1.8752 \pm 0.0036) \times 10^{16}$	$(1.1762 \pm 0.0013) \times 10^{18}$
G-03-0291-LH	$(7.4875 \pm 0.0098) \times 10^{16}$	$(7.8964 \pm 0.0098) \times 10^{18}$	$(1.7218 \pm 0.0035) \times 10^{15}$	$(7.2424 \pm 0.0080) \times 10^{17}$
G-03-0291-CWD	$(5.2837 \pm 0.0075) \times 10^{16}$	$(5.5700 \pm 0.0069) \times 10^{18}$	$(1.2130 \pm 0.0084) \times 10^{15}$	$(5.1105 \pm 0.0056) \times 10^{17}$

Uncertainties represent expanded uncertainties with a coverage factor of $k = 2$

Table 5 Concentration of progeny isotopes in the primary dissolution solution on a reference date of February 2, 2017

Sample ID	^{231}Pa (atoms g^{-1})	^{230}Th (atoms g^{-1})	^{227}Ac (atoms g^{-1})	^{226}Ra (atoms g^{-1})
G-03-0146-LH	$(3.540 \pm 0.046) \times 10^{12}$	$(7.865 \pm 0.038) \times 10^{13}$	$(1.439 \pm 0.054) \times 10^{9}$	$(2.176 \pm 0.054) \times 10^{10}$
G-03-0146-CWD	$(5.388 \pm 0.070) \times 10^{12}$	$(1.4566 \pm 0.0071) \times 10^{14}$	$(2.64 \pm 0.10) \times 10^{9}$	$(3.790 \pm 0.094) \times 10^{10}$
G-03-0291-LH	$(5.491 \pm 0.071) \times 10^{12}$	$(1.5210 \pm 0.0074) \times 10^{14}$	$(1.599 \pm 0.061) \times 10^{9}$	$(2.560 \pm 0.064) \times 10^{10}$
G-03-0291-CWD	$(4.150 \pm 0.054) \times 10^{12}$	$(1.1738 \pm 0.0058) \times 10^{14}$	$(1.122 \pm 0.043) \times 10^{9}$	$(1.264 \pm 0.032) \times 10^{10}$

Table 6 Atom ratio of progeny isotopes to parent isotopes in the ^{235}U decay series on February 2, 2017

Sample ID	$^{231}Pa/^{235}U$	$^{227}Ac/^{235}U$	$^{227}Ac/^{231}Pa$
G-03-0146-LH	$(4.504 \pm 0.059) \times 10^{-7}$	$(1.834 \pm 0.070) \times 10^{-10}$	$(4.07 \pm 0.16) \times 10^{-4}$
G-03-0146-CWD	$(3.619 \pm 0.048) \times 10^{-7}$	$(1.778 \pm 0.067) \times 10^{-10}$	$(4.91 \pm 0.20) \times 10^{-4}$
G-03-0291-LH	$(6.953 \pm 0.091) \times 10^{-7}$	$(2.028 \pm 0.077) \times 10^{-10}$	$(2.92 \pm 0.12) \times 10^{-4}$
G-03-0291-CWD	$(7.451 \pm 0.098) \times 10^{-7}$	$(2.018 \pm 0.077) \times 10^{-10}$	$(2.71 \pm 0.11) \times 10^{-4}$

Table 7 Atom ratio of progeny isotopes to parent isotopes in the ^{234}U decay series on February 2, 2017

Sample ID	$^{230}Th/^{234}U$	$^{226}Ra/^{234}U$	$^{226}Ra/^{230}Th$
G-03-0146-LH	$(1.2981 \pm 0.0075) \times 10^{-3}$	$(3.592 \pm 0.090) \times 10^{-7}$	$(2.767 \pm 0.070) \times 10^{-4}$
G-03-0146-CWD	$(1.2683 \pm 0.0075) \times 10^{-3}$	$(3.300 \pm 0.083) \times 10^{-7}$	$(2.602 \pm 0.066) \times 10^{-4}$
G-03-0291-LH	$(2.031 \pm 0.011) \times 10^{-3}$	$(3.419 \pm 0.086) \times 10^{-7}$	$(1.683 \pm 0.043) \times 10^{-4}$
G-03-0291-CWD	$(2.222 \pm 0.013) \times 10^{-3}$	$(2.392 \pm 0.060) \times 10^{-7}$	$(1.076 \pm 0.027) \times 10^{-4}$

isotopes were preferentially sequestered into the solid heel material relative to their parent U isotopes.

In order to extract useful age information from the results obtained, it is necessary to develop a decay model to predict how the granddaughter/daughter ratios (i.e. $^{227}Ac/^{231}Pa$ and $^{226}Ra/^{230}Th$) evolve with time during radioactive decay (Fig. 3). It is assumed that when initially filled, the UF_6 cylinders contain only U isotopes and no progeny isotopes. Thus, the U decay series can be modelled using Bateman's equations of radioactive decay [1] without the need to account for the presence of progeny isotopes at $t = 0$. The radioactive decay constants used to construct the decay models are $\lambda_{235} = (9.8485 \pm 0.0135) \times 10^{-10}$ years (2σ), $\lambda_{234} = (2.8263 \pm 0.0056) \times 10^{-6}$ years (2σ),

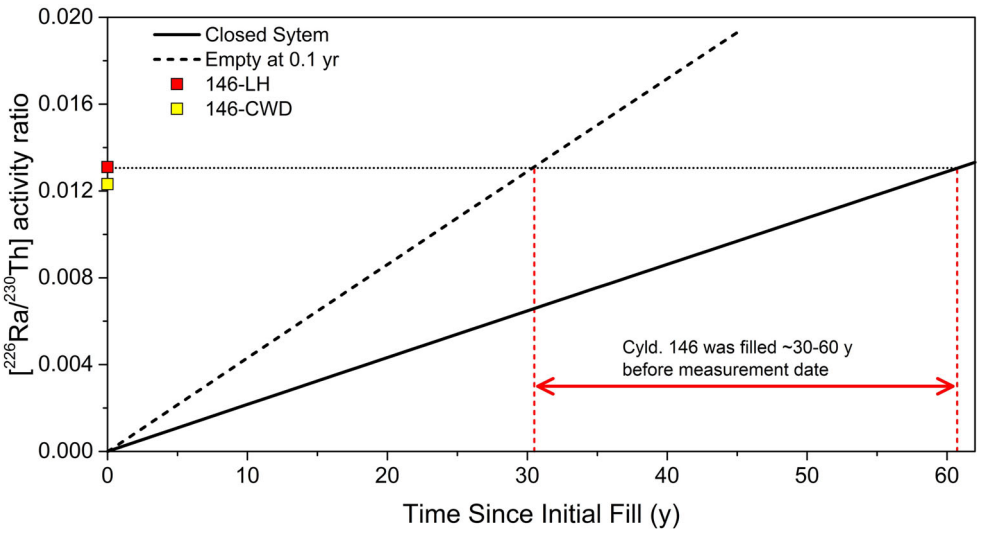

Fig. 3 Modelled evolution of the $^{226}Ra/^{230}Th$ activity ratio through time considering the two boundary conditions of (1) closed system and (2) removal of all U after some $t > 0$. The two data points are the $^{226}Ra/^{230}Th$ ratios determined for samples G-03-0146-LH and G-03-0146-CWD. Based on sample G-03-0146-LH, the model predicts the cylinder G-03-0146 was initially filled between 30 and 60 years before the sample analyses in 2017

$\lambda_{231} = (2.1158 \pm 0.0071) \times 10^{-5}$ years (2σ), $\lambda_{230} = (9.158 \pm 0.028) \times 10^{-6}$ years (2σ), $\lambda_{227} = (3.184 \pm 0.001) \times 10^{-2}$ years (2σ), and $\lambda_{226} = (4.332 \pm 0.019) \times 10^{-4}$ years (2σ) [8–10].

Using the ^{234}U–^{230}Th–^{226}Ra system as the primary example, the decay of ^{234}U to ^{230}Th to ^{226}Ra results in a $^{226}Ra/^{230}Th$ ratio that is determined by the (1) amount of time that has passed since the U was last purified and (2) whether or not the system has remained closed such that no material (i.e. progeny or parent isotopes) has been added or removed. Two boundary conditions can then be imagined with the first being a closed system where the ^{234}U is allowed to decay unimpeded which thereby continues to support the decay of ingrown ^{230}Th which in turn supports the decay of ingrown ^{226}Ra (Fig. 3; solid line). The second boundary condition is one in which some amount of time passes (i.e. $t > 0$) to allow for a small amount of ingrown ^{230}Th and ^{226}Ra to accumulate before the bulk of the ^{234}U is removed from the system. In the model presented here, the U is removed at 0.1 year (Fig. 3; dashed line) but could be modelled as being removed at some infinitesimally small amount of time. It is clear from Fig. 3 that the two boundary conditions result in significantly different trajectories in the $^{226}Ra/^{230}Th$ ratios. This result is due to the fact that the decay of ingrown ^{230}Th is no longer supported by the decay of ^{234}U once all of the U has been removed from the system which results in a significant increase in the $^{226}Ra/^{230}Th$ ratio over time compared to a closed system model. Under these boundary conditions, the age of a UF_6 cylinder can be estimated to within a certain range. In the case of sample G-03-0146-LH, the $^{226}Ra/^{230}Th$ age is between ~ 30 and 60 years (Fig. 3).

Since the history of cylinders G-03-0146 and G-03-0291 are reasonably well known, it is possible to constrain the model further (Fig. 4). It is known that the cylinders were emptied of nearly all of their remaining UF_6 around January 2012 at NFS (Table 1). The $^{226}Ra/^{230}Th$ as measured on February 2, 2017 can be decay-corrected to the date on which the cylinders were reportedly emptied by assuming unsupported decay of ^{230}Th between the time the cylinder was fully emptied and the time the measurements were made. If cylinder G-03-0146 had remained a closed system between the time it was initially filled and the time that it was emptied in 2012, then the decay-corrected $^{226}Ra/^{230}Th$ ratio for sample G-03-0146-LH (green circle in Fig. 4) should fall on the 'closed system' line in Fig. 4. However, it is known that only ~ 10 g of UF_6 was removed from cylinder G-03-0146 in 2012, indicating that the cylinder must have been essentially emptied prior to 2012. Therefore, it is not expected that the decay-corrected $^{226}Ra/^{230}Th$ ratio should fall on the 'closed system' line. As can be seen in Fig. 4, the decay-corrected $^{226}Ra/^{230}Th$ ratio (green circle) does not fall on the 'closed system' line, in agreement with the knowledge that it was emptied prior to 2012. For completeness, the red solid line ('Empty at 35 years') in Fig. 4 demonstrates the trajectory of the $^{226}Ra/^{230}Th$ ratio had the cylinder remained closed up until 2012 before being fully emptied. This model of a closed system between the time the cylinder was initially filled in 1977 and when it was emptied in 2012 does not fit the data. The simplest fit of the model to the observed $^{226}Ra/^{230}Th$ ratio for sample G-03-0146-LH is found for the cylinder remaining a closed system between its fill date in 1977 and the cylinder being fully emptied in 1995, ca 17.5 years after its initial fill date in 1977 (Fig. 4; blue dashed line). A similar model fit is found for sample G-03-0146-CWD (not shown). However, it is known that cylinder G-03-0146 was used as an analytical standard after its initial fill date, and therefore aliquots of UF_6 would have been removed from time to time, thereby affecting the trajectory of the

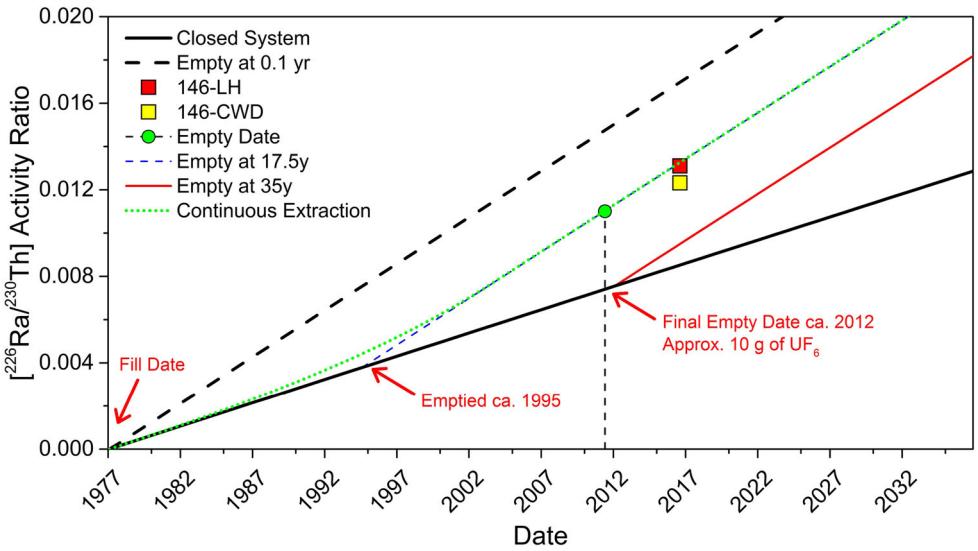

Fig. 4 Modelled evolution of the $^{226}Ra/^{230}Th$ activity ratio through time for cylinder G-03-0146. The two boundary conditions are the same as in Fig. 3. The additional lines represent different scenarios for when the cylinder was emptied of its UF_6. The measured data are the red and yellow squares. The green circle is the decay-corrected $^{226}Ra/^{230}Th$ ratio for G-03-0146-LH. See text for details. (Color figure online)

$^{226}Ra/^{230}Th$ ratio due to the gradual reduction in the support of decaying ^{230}Th from the decay of ^{234}U. The green dashed line in Fig. 4 demonstrates how continuously extracting UF_6 at a rate of $\sim$ 3.75% of the starting amount per year for 25 years (1977–2002) alters the trajectory of the $^{226}Ra/^{230}Th$ ratio. As UF_6 is continually removed from the system and is ultimately emptied, the trajectory of the $^{226}Ra/^{230}Th$ ratio gradually steepens until its slope matches the slope of the trajectory of a fully emptied cylinder due to the unsupported decay of ^{230}Th. Thus, there are multiple scenarios under which the observed $^{226}Ra/^{230}Th$ ratio could be generated. That is, as long as a model can be generated that passes through the decay-corrected $^{226}Ra/^{230}Th$ ratio (green circle in Fig. 4), then the model is deemed successful at fitting the observed data. In the case of cylinder G-03-0146, the model demonstrates that the cylinder could not have been fully emptied before 1995, but that it could have been partially emptied over the course of the working lifetime of the cylinder before it was fully emptied at some time between 1995 and 2012.

The conclusions reached with the ^{234}U–^{230}Th–^{226}Ra decay chain can also be drawn from the ^{235}U–^{231}Pa–^{227}Ac decay chain for cylinder G-03-0146 using the same model parameters (Fig. 5). However, the $^{227}Ac/^{231}Pa$ ratio for sample G-03-0146-CWD is not in agreement with sample G-03-0146-LH or with the $^{226}Ra/^{230}Th$ data. There is an elevated $^{227}Ac/^{231}Pa$ ratio for sample G-03-0146-CWD (Fig. 5) which appears to be related to a deficit in the measured ^{231}Pa concentration rather than an excess in the ^{227}Ac concentration, judging by the $^{231}Pa/^{235}U$ and $^{227}Ac/^{235}U$ ratios in samples G-03-0146-CWD compared to G-03-0146-LH (Table 6). In other words, the $^{231}Pa/^{235}U$ in sample G-03-146-CWD is $\sim$ 20% lower than the $^{231}Pa/^{235}U$ ratio in sample G-03-146-LH, whereas there is only an $\sim$ 3% difference in the $^{227}Ac/^{235}U$ ratios between samples G-03-146-CWD and G-03-146-LH. The source of this disagreement is not yet known but, as will be shown below, there is also a disagreement between the loose heels and the cylinder wall deposits with respect to the $^{226}Ra/^{230}Th$ ratios determined for sample G-03-0291. The two cylinder wall deposit samples that are in disagreement actually lie outside the boundary conditions of the model which indicate the model assumptions are not being met for these two samples. Such disagreement may indicate that the cylinder was previously used for a different UF_6 material that had a different U isotope composition from the UF_6 that the loose heel material formed from or that there could be elemental fractionation between the progeny isotopes during the formation of corrosive wall deposits. It is unclear as to whether cylinders G-03-0146 and G-03-0291 were new when they were initially filled at PORTS.

Cylinder G-03-0291 was also emptied by NFS in 2012 but at the time of emptying it contained $\sim$ 1 kg of UF_6, significantly more than contained in cylinder G-03-0146 ($\sim$ 10 g) when it was emptied. Due to this, the decay-corrected $^{226}Ra/^{230}Th$ ratio (green circle in Fig. 6) is much closer to the ratio predicted by a closed system model (black solid line in Fig. 6), but it is still not a perfect match. This likely indicates that the cylinder remained nearly full between the time it was filled in 1987 until the time it was emptied in 2012. In the case of cylinder G-03-0291, the data for sample G-03-0291-LH is most simply fit by a model that behaves as a closed system from the initial fill date in 1987 up until it was fully emptied in ca. 2010 (blue dashed line in Fig. 6). More likely though is a more complex scenario that allows for the removal of some UF_6 prior to the cylinder being fully emptied in 2012 ($\sim$ 2.4% of starting amount removed per year; green dashed line Figs. 6, 7). As mentioned above, there is disagreement between the $^{226}Ra/^{230}Th$ ratios measured for samples G-03-

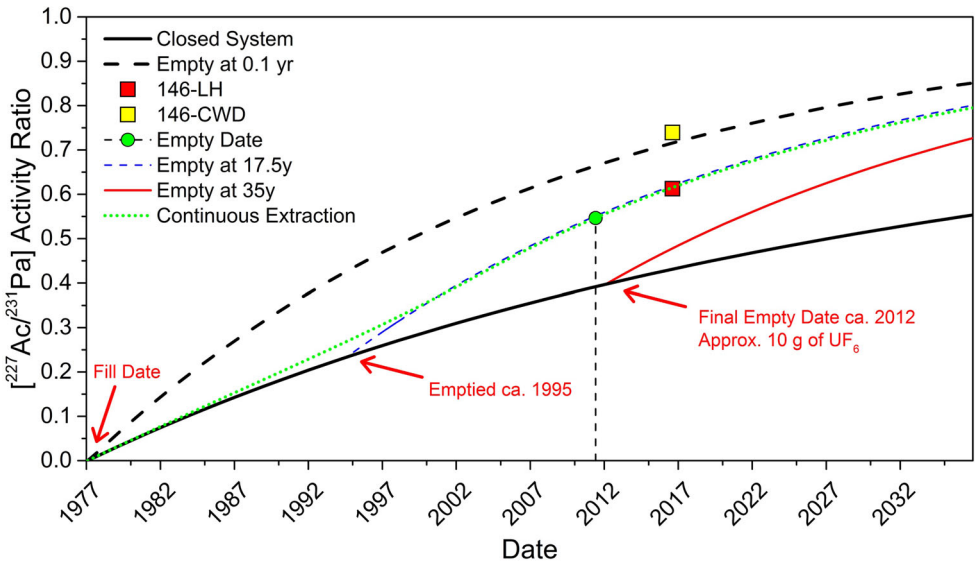

Fig. 5 Modelled evolution of the $^{227}Ac/^{231}Pa$ activity ratio through time for cylinder G-03-0146. Model parameters are identical to Fig. 4 except for now the ^{235}U–^{231}Pa–^{227}Ac decay chain is being modelled. The measured data are the red and yellow squares. The green circle is the decay-corrected $^{227}Ac/^{231}Pa$ ratio for G-03-0146-LH. (Color figure online)

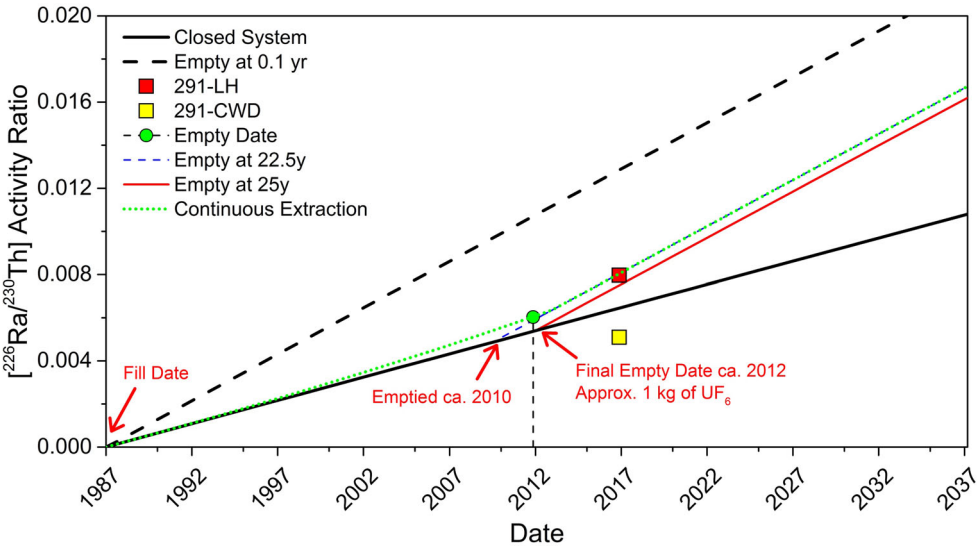

Fig. 6 Modelled evolution of the $^{226}Ra/^{230}Th$ activity ratio through time for cylinder G-03-0291. Model is identical to Fig. 4 but now the dates on which the cylinder was emptied have been modified. The measured data are the red and yellow squares. The green circle is the decay-corrected $^{226}Ra/^{230}Th$ ratio for G-03-0291-LH. (Color figure online)

0291-LH and G-03-0291-CWD. In this case it appears that sample G-03-0291-CWD suffers from both an excess of ^{230}Th of $\sim$ 10% and a deficit of ^{226}Ra of $\sim$ 30%, judging by the difference in the measured $^{230}Th/^{234}U$ and $^{226}Ra/^{234}U$ ratios in G-03-0291-CWD when compared to G-03-0291-LH (Table 7). Furthermore, the model parameters used to fit model to the measured $^{226}Ra/^{234}U$ ratio in sample G-03-0291-LH also provide a satisfactory fit of the model to the measured $^{227}Ac/^{231}Pa$ ratios in both samples G-03-0291-LH and G-03-0291-CWD (Fig. 7), which increases overall confidence in the quality and interpretation of the data.

Conclusions and outlook

It has been demonstrated that the progeny isotopes in the U decay series are preferentially sequestered into the solid heel material that forms inside UF_6 storage cylinders which does not sublimate as UF_6 does. Because the progeny isotopes are preferentially enriched in the solid heel material relative to U, radiometric dating of this material resulted in ages that were unrealistically old based on the ^{231}Pa–^{235}U and ^{230}Th–^{234}U radiochronometers. In order to circumvent this issue, ^{227}Ac and ^{226}Ra, which are the granddaughter isotopes in the ^{235}U–^{231}Pa–^{227}Ac and ^{234}U–^{230}Th–^{226}Ra decay chains, were also analyzed. It was found that the $^{227}Ac/^{231}Pa$ and $^{226}Ra/^{230}Th$ ratios in the heel material evolve as a function of time and that a range of radiometric model ages of the initial cylinder fill date

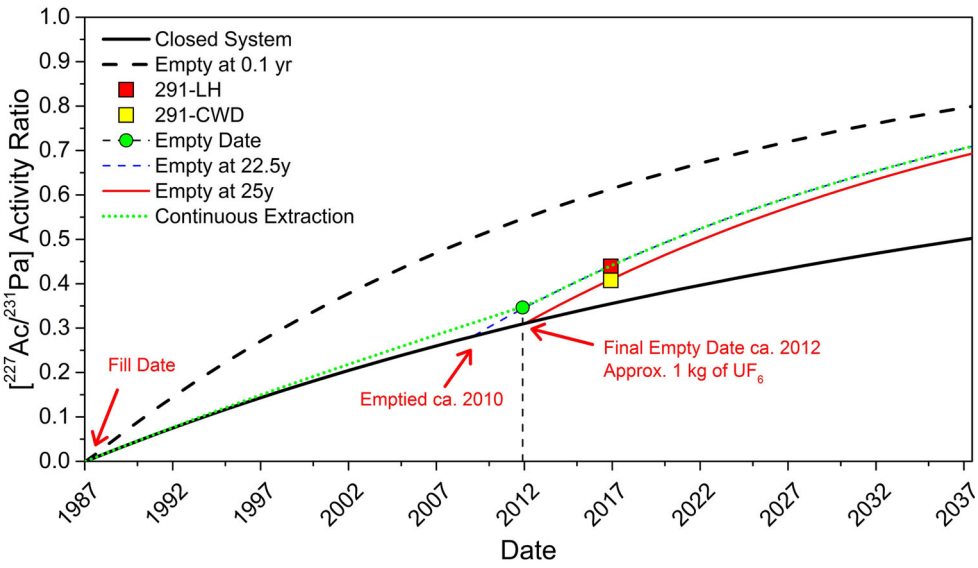

Fig. 7 Modelled evolution of the $^{227}Ac/^{231}Pa$ activity ratio through time for cylinder G-03-0146. Model parameters are identical to Fig. 6 except for now the ^{235}U–^{231}Pa–^{227}Ac decay chain is being modelled. The measured data are the red and yellow squares. The green circle is the decay-corrected $^{227}Ac/^{231}Pa$ ratio for G-03-0291-LH. (Color figure online)

can be determined based on boundary conditions imposed on the model. However, the range in the possible age of the cylinders determined in this manner is quite large and thus it is not likely to result in precise fill dates of the cylinders. However, this method could be useful for validating the declared history of cylinders in a verification scenario. For instance, if a cylinder was declared to have been filled and emptied on certain dates, then a model can be constructed for the evolution of the $^{227}Ac/^{231}Pa$ and $^{226}Ra/^{230}Th$ ratios through time that would necessarily match the measured $^{227}Ac/^{231}Pa$ and $^{226}Ra/^{230}Th$ ratios in the heel material. Disagreement between the modelled $^{227}Ac/^{231}Pa$ and $^{226}Ra/^{230}Th$ ratios and the measured $^{227}Ac/^{231}Pa$ and $^{226}Ra/^{230}Th$ ratios may then indicate that the declared history of the cylinder is inaccurate.

Acknowledgements This work was performed under the auspices of the U.S. Department of Energy by Lawrence Livermore National Laboratory under Contract No. DE-AC52-07NA27344. Funding was provided by the United States Department of Homeland Security's Domestic Nuclear Detection Office through the National Nuclear Forensics Expertise Development Program. The views and conclusions contained in this document are those of the authors and should not be interpreted as representing the official policies, either expressed or implied, of the U.S. Department of Homeland Security. LLNL-JRNL-747574.

References

1. Bateman H (1910) Solution of a system of differential equations occurring in the theory of radioactive transformations. Proc Camb Philos Soc 15:423
2. Eppich GR, Williams RW, Gaffney AM, Schorzman KC (2013) ^{235}U–^{231}Pa age dating of uranium materials for nuclear forensic investigations. J Anal At Spectrom 28:666–674
3. Williams RW, Gaffney AM (2011) ^{230}Th–^{234}U model ages of some uranium standard reference materials. Proc Radiochim Acta 1:31–35
4. Kayzar TM, Williams RW (2016) Developing ^{226}Ra and ^{227}Ac age-dating techniques for nuclear forensics to gain insight from concordant and non-concordant radiochronometers. J Radioanal Nucl Chem 307:2061–2068
5. Rolison JM, Trienen KC, McHugh KC, Gaffney AM, Williams RW (2017) Application of the ^{226}Ra–^{230}Th–^{234}U and ^{227}Ac–^{231}Pa–^{235}U radiochronometers to uranium certified reference materials. J Radioanal Nucl Chem 314:2459–2467
6. United States Enrichment Corporation (1995) Uranium hexafluoride: a manual of good handling practices. Revision 7. United States. https://doi.org/10.2172/205924
7. Munday E, Bostick W, Wagner G (2013) Sampling of five type 2S uranium hexafluoride (UF_6) cylinders from nuclear fuel services. Materials and Chemistry Laboratory, Inc. Project UTB002606
8. Cheng H, Edwards RL, Hoff J, Gallup CD, Richards DA, Asmerom Y (2000) The half-lives of uranium-234 and thorium-230. Chem Geol 169:17–33
9. Jaffey AH, Flynn KF, Glendenin LE, Bentley WC, Essling AM (1971) Precision measurement of half-lives and specific activities of 235U and 238U. Phys Rev C 4:1889–1906
10. IAEA (2004) Handbook of nuclear data for safeguards: database extensions, August 2008. International Nuclear Data Committee INDC (NDS)-0534